Published Ahead of Print on September 12, 2022 as 10.1212/WNL.0000000000201264

Neurology®

The most widely read and highly cited peer-reviewed neurology journal
The Official Journal of the American Academy of Neurology

AMERICAN ACADEMY OF NEUROLOGY®

Neurology Publish Ahead of Print
DOI: 10.1212/WNL.0000000000201264

Investigating Functional Network Abnormalities and Associations With Disability in Multiple Sclerosis

Author(s):
Antonio Carotenuto, MD[1]; Paola Valsasina, MSc[1]; Menno M. Schoonheim, PhD[2]; Jeroen JG Geurts, PhD[2]; Frederik Barkhof, MD, PhD[3,4,5]; Antonio Gallo, MD, PhD[6]; Gioacchino Tedeschi, MD[6]; Silvia Tommasin, PhD[7]; Patrizia Pantano, MD[7,8]; Massimo Filippi, Professor, MD[1,9,10,11,12]; Maria A. Rocca, MD[1,9,12] on behalf of MAGNIMS Study Group

Corresponding Author:
Maria A. Rocca, rocca.mara@hsr.it

Affiliation Information for All Authors: 1.Neuroimaging Research Unit, Division of Neuroscience, IRCCS San Raffaele Scientific Institute, Milan, Italy; 2.Department of Anatomy and Neurosciences, MS Center Amsterdam, Amsterdam Neuroscience, Amsterdam UMC, Vrije Universiteit Amsterdam, Amsterdam, The Netherlands; 3.Radiology and Nuclear Medicine, MS Center Amsterdam, Amsterdam Neuroscience, Amsterdam UMC, Vrije Universiteit Amsterdam, Amsterdam, The Netherlands; 4.Institutes of Neurology & Healthcare Engineering, UCL, London, UK; 5.National Institute for health research (NIHR) University College London Hospitals (UCLH) Biomedical research centre, London, UK; 6.Division of Neurology and 3T MRI Research Center, Department of Advanced Medical and Surgical Sciences, University of Campania "Luigi Vanvitelli", Naples, Italy; 7.Department of Human Neurosciences, Sapienza University, Rome, Italy; 8.IRCCS NEUROMED, Pozzilli (IS), Italy; 9.Neurology Unit, IRCCS San Raffaele Scientific Institute, Milan, Italy; 10.Neurorehabilitation Unit, IRCCS San Raffaele Scientific Institute, Milan, Italy; 11.Neurophysiology Service, IRCCS San Raffaele Scientific Institute, Milan, Italy; 12.Vita-Salute San Raffaele University, Milan, Italy

Equal Author Contribution:

Contributions:
Antonio Carotenuto: Drafting/revision of the manuscript for content, including medical writing for content; Analysis or interpretation of data
Paola Valsasina: Drafting/revision of the manuscript for content, including medical writing for content; Analysis or interpretation of data
Menno M. Schoonheim: Drafting/revision of the manuscript for content, including medical writing for content; Major role in the acquisition of data; Analysis or interpretation of data
Jeroen JG Geurts: Drafting/revision of the manuscript for content, including medical writing for content; Major role in the acquisition of data
Frederik Barkhof: Drafting/revision of the manuscript for content, including medical writing for content; Major role in the acquisition of data
Antonio Gallo: Drafting/revision of the manuscript for content, including medical writing for content; Major role in the acquisition of data
Gioacchino Tedeschi: Drafting/revision of the manuscript for content, including medical writing for content; Major role in the acquisition of data
Silvia Tommasin: Drafting/revision of the manuscript for content, including medical writing for content; Major role in the acquisition of data
Patrizia Pantano: Drafting/revision of the manuscript for content, including medical writing for content; Major role in the acquisition of data; Analysis or interpretation of data
Massimo Filippi: Drafting/revision of the manuscript for content, including medical writing for content; Analysis or interpretation of data
Maria A. Rocca: Drafting/revision of the manuscript for content, including medical writing for content; Study concept or design; Analysis or interpretation of data; Additional contributions: Study supervisor.

Figure Count:
2

Table Count:
5

Search Terms:
[41] Multiple sclerosis, [120] MRI, [121] fMRI

Acknowledgment:

Study Funding:
Antonio Carotenuto was supported by a MAGNIMS/ECTRIMS research fellowship programme. Frederik Barkhof is supported by the NIHR biomedical research center at UCLH.

Disclosures:
A. Carotenuto received research grants from ALMIRALL, and honoraria form Novartis, Merck, and Biogen; P. Valsasina received speaker honoraria from Biogen Idec; M.M. Schoonheim serves on the editorial boards of Neurology and Frontiers in Neurology, receives research support from the Dutch MS Research Foundation and has served as a consultant for or received research support from Atara Biotherapeutics, Biogen, Celgene, Genzyme, MedDay and Merck; J.J.G. Geurts has served as a consultant for or received research support from Biogen, Celgene, Genzyme, MedDay, Merck, Novartis and Teva; F. Barkhof serves as an Editorial Board member of Radiology, Neurology, Multiple Sclerosis Journal and Neuroradiology; he has accepted consulting fees from Biogen-IDEC, IXICO Ltd, Jansen, Merck Serono, Novartis, Roche, and Combinostics.; A. Gallo received speaker and consulting fees from Biogen, Genzyme, Merck Serono, Mylan, Novartis, Roche, and Teva, and receives research support from Fondazione Italiana Sclerosi Multipla; G. Tedeschi received consulting fees and research support from Biogen, Genzyme, Merck Serono, Mylan, Novartis, Roche, Teva, Allergan, Abbvie and Lundbeck; S. Tommasin received speaker fees from Roche. P. Pantano received founding for travel from Novartis, Genzyme, Bracco, and Biogen; M. Filippi is Editor-in-Chief of the Journal of Neurology and Associate Editor of Human Brain Mapping; received compensation for consulting services and/or speaking activities from Almiral, Alexion, Bayer, Biogen, Celgene, Eli Lilly, Genzyme, Merck-Serono, Novartis, Roche, Sanofi, Takeda, and Teva Pharmaceutical Industries; and receives research support from Biogen Idec, Merck-Serono, Novartis, Roche, Teva Pharmaceutical Industries, Italian Ministry of Health, Fondazione Italiana Sclerosi Multipla, and ARiSLA (Fondazione Italiana di Ricerca per la SLA); M.A. Rocca received speaker honoraria from Bayer, Biogen, Bristol Myers Squibb, Celgene, Genzyme, Merck Serono, Novartis, Roche, and Teva, and receives research support from the MS Society of Canada and Fondazione Italiana Sclerosi Multipla.

Preprint DOI:

Received Date:
2022-03-09

Accepted Date:
2022-08-01

Handling Editor Statement:
Submitted and externally peer reviewed. The handling editor was Elizabeth Silbermann, MD.

Abstract

Background and Objectives: In multiple sclerosis (MS), functional networks undergo continuous reconfiguration and topography changes over the disease course. Here, we aimed to investigate functional networks topography abnormalities in MS and their association with disease phenotype, clinical and cognitive disability, and structural MRI damage.

Methods: This is a multi-centre cross-sectional study. Enrolled subjects performed MRI, neurological and neuropsychological assessment. Network topography was assessed on resting state fMRI data using degree centrality, which counted the number of functional connections of each grey matter voxel with the rest of the brain. SPM12 age-, sex-, scanner-, framewise displacement and grey matter volume adjusted ANOVA and multivariable regressions were employed ($p<0.05$, family-wise error [FWE] corrected).

Results: We enrolled 971 patients with MS (624 females; mean age=43.1 ±11.8 years; 47 clinically isolated syndrome [CIS], 704 relapsing-remitting [RRMS], 145 secondary progressive [SPMS] and 75 primary progressive [PPMS]) and 330 healthy controls (186 females; mean age=41.2 ± 13.3 years). Patients with MS showed reduced centrality in the salience and sensorimotor networks as well as increased centrality in the default mode network *vs* controls ($p<0.05$, FWE). Abnormal centrality was already found in CIS *vs* controls and in RRMS *vs* CIS ($p<0.001$, uncorrected); however it became more severe in SPMS *vs* RRMS ($p<0.05$, FWE) and in PPMS *vs* controls ($p<0.001$, uncorrected). Cognitively impaired patients (39%) showed reduced centrality in the salience network and increased centrality in the default mode network *vs* cognitively preserved patients ($p<0.001$, conjunction analysis). More severe disability correlated with increased centrality in the right precuneus ($r=0.18$, $p<0.05$ FWE). Higher T2 lesion volume and brain/grey matter atrophy were associated with reduced centrality in the bilateral insula and cerebellum (r=range -0.17/-0.15 and 0.26/0.28, respectively; $p<0.05$, FWE). Higher brain/grey matter atrophy was also associated with increased centrality in the default mode network (r=range -0.31/-0.22, $p<0.05$, FWE).

Discussion: Patients with MS presented with reduced centrality in the salience and primary sensorimotor networks and increased centrality in the default mode network. Centrality abnormalities were specific for different disease phenotypes and associated with clinical and cognitive disability, hence suggesting that voxel-wise centrality analysis may reflect pathological substrates underpinning disability accrual.

Introduction

Multiple sclerosis (MS) is a chronic inflammatory, demyelinating and neurodegenerative CNS disorder characterised by considerable inter-individual variability in terms of disease presentation and clinical course,[1] and quite different rates of accumulation of physical disability and cognitive impairment across subjects.[2] A variable amount and efficiency of functional reserve and plasticity mechanisms across disease stages is likely to play a role for inter-individual disease severity differences.[3]

Despite its great sensitivity in detecting focal white matter damage, conventional MRI only partly explains clinical disability at a subject-level.[4] To overcome this gap, MRI assessment has shifted from measuring local tissue alterations to evaluating how the brain responds to such damage with reconfiguration of neuronal connections and brain networks. Resting state functional connectivity allows depicting the extent of global communication and integration of information among networks, by assessing the spatio-temporal coherence of time-dependent blood oxygenation level-dependent signal across brain areas.[5] Previous studies mostly reported an overall increased resting state functional connectivity of large-scale brain networks in the earliest phases of MS, followed by reduced connectivity later in the disease course all of which have mostly been related to worse clinical functioning.[6-8] While being informative of the within- and between-network functional status, conventional analysis of large-scale networks does not investigate integrity of whole-network topography and architecture. To overcome this limit, graph analysis has been applied to resting state fMRI. Graph analysis is a theoretical framework investigating networks topography through different metrics (i.e., path length, modularity, hubness, etc.).[9] One of the key graph theory

metrics is centrality, a measure of the relative importance of individual brain regions over the whole-brain network and hence, a measure of hubness.[10] Recently, the possibility to assess centrality (in particular, degree centrality or eigenvector centrality[10]) at a voxel-wise level has fostered the analysis of network topography abnormalities in MS without the need to parcellate brain areas and to select region of interests, helping scientists to further track network reorganization over the disease course. Previous studies exploring voxel-wise centrality abnormalities in patients with MS reported increased centrality in regions belonging to the default mode and basal ganglia networks, as well as reduced centrality in the sensorimotor network and ventral stream areas.[11-14] However, recent findings in MS also suggested disease stage-specific network changes.[15] A comprehensive characterization of centrality abnormalities across disease phenotypes (i.e., clinically isolated syndrome [CIS], relapsing-remitting MS [RRMS], secondary progressive MS [SPMS] and primary progressive MS [PPMS]) has been hampered so far by the lack of large enough samples sizes. This may also explain inconsistent results about centrality abnormalities with regards to clinical disability,[11, 13] cognitive deficits[11, 12, 16] or structural MRI abnormalities.[14]

Against this background, we assessed voxel-wise centrality abnormalities in a large sample of patients with MS spanning the different disease clinical phenotypes in a multicentre collaboration. We aimed to investigate associations of centrality abnormalities with clinical disability and cognitive impairment as well as with structural MRI measures, namely T2 lesion volume and brain/grey matter atrophy. In line with previous reports,[11-16] we anticipated overall increased centrality in the default-mode network and decreased centrality in sensorimotor areas in patients with MS, becoming more evident in progressive phenotypes. We also hypothesised that centrality abnormalities associate with structural damage and parallel clinical and cognitive disability.

Methods

Subjects

This was a multi-centre, cross-sectional study at four European centres from the Magnetic Resonance Imaging in Multiple Sclerosis consortium (magnims.eu): 1) the Neuroimaging Research Unit, IRCCS San Raffaele Scientific Institute, Milan (Italy); 2) the MS Center Amsterdam, Amsterdam UMC, location VUmc, Amsterdam (the Netherlands); 3) the MRI Center 'SUN-FISM', University of Campania 'Luigi Vanvitelli', Naples (Italy); 4) Department of Human Neurosciences, Sapienza University, Rome, Italy.

We included subjects satisfying the following inclusion criteria: 1) right-handedness, to avoid between-subject variability according to brain functional lateralization;[17, 18] 2) no history of significant medical illnesses or substance abuse; 3) no other major systemic, psychiatric or neurological diseases; and 4) no contraindications to MRI (claustrophobia, pregnancy or breastfeeding). We included both healthy controls (hereafter labelled as 'controls') and patients with MS according to 2017 McDonald criteria.[19] Patients with MS had to be relapse- and steroid-free for at least one month before MRI acquisition and have a stable disease-modifying treatment from at least 6 months.

Standard Protocol Approvals, Registrations, and Patient Consents

Approval was received from the local ethical committee (IRCCS San Raffaele Scientific Institute, Milan, Italy; protocol ID: "Centrality-MS") All subjects gave written informed consent prior to study participation. The study was performed in accordance with good clinical practices and the Declaration of Helsinki. A MAGNIMS data-sharing agreement was signed among the participating centres.

Clinical and neuropsychological assessment

Within 2 days from MRI scanning, patients with MS underwent a clinical examination, including the assessment of the Expanded Disability Status Scale (EDSS).[20] Patients with MS and controls underwent a neuropsychological assessment including the following tests embedded in the brief

repeatable battery of neuropsychological tests[2]: the selective reminding test to assess verbal memory, the 10/36 spatial recall test to assess visuo-spatial memory; the symbol digit modalities test to assess attention and information processing speed; and the word list generation test to assess verbal fluency. Scores at each test were Z-converted either using age-, sex- and education- adjusted normative values[21] for the Italian centres or by subtracting the mean performance and dividing by the SD of controls after correction for age, sex and education for the Amsterdam centre. Patients were classified as cognitively impaired if Z-scores fell below 1.5 SDs on at least 2 tests, cognitively preserved otherwise.[22]

MRI acquisition

All subjects underwent a brain MRI scan using a 3.0 T system at all sites (IRCCS San Raffaele Scientific Institute: Scanner I: Philips Achieva; Scanner II: Philips Ingenia; Amsterdam UMC and University of Campania "L. Vanvitelli", Naples: General Electric Signa HDtx; Sapienza University: Siemens Magnetom Verio), including the following sequences: (1) Resting state fMRI, using a T2*-weighted echo planar imaging sequence (repetition time=range 1508-3000 ms; in-plane spatial resolution=range 1.87x1.87-4x4 mm^2; slice thickness=range 3-4 mm; number of acquired scans=range 140-320). During resting state fMRI, subjects were instructed to keep their eyes closed, to remain motionless and not to think of anything in particular. All subjects reported that they had not fallen asleep during scanning, according to a questionnaire delivered immediately after the MRI session; (2) variable flip angle three-dimensional (3D) fluid attenuated inversion recovery or 2D dual echo turbo spin echo for T2 lesion assessment; and (3) 3D T1-weighted turbo field echo sequence (inversion prepared, spatial resolution≅1x1x1 mm^3) for resting state fMRI pre-processing and atrophy assessment.

Structural MRI analysis

Focal white matter lesions were identified on 3D fluid attenuated inversion recovery /3D T1-weighted MRI sequences using a fully automated approach based on a cascade of two 3D patch-wise convolutional neural networks,[23] or on dual echo turbo spin echo scans using a semi-

automated method implemented in Jim 7.0 (Xinapse Systems, Colchester, UK). Then, total T2-hyperintense lesion volume was obtained. Normalised brain and grey matter volume was calculated using FSL SIENAx software on the lesion-filled[24] 3D T1-weighted images.

Resting state fMRI analysis: pre-processing

Resting state fMRI data processing was performed using the CONN toolbox.[25] Resting state fMRI images were realigned to the mean of each session using a rigid-body transformation to correct for head movements. The mean framewise displacement[26] was calculated as a measure of movement; subjects presenting with a framewise displacement higher than 0.5 mm[26] were excluded from the analysis. After rigid registration of realigned images to the lesion filled 3D T1-weighted scan, resting state fMRI images were normalised to the Montreal Neurological Institute space using a non-linear transformation. After visual check of registration outputs and detection of outliers (using the ART tool), images were smoothed with a 6-mm^3 Gaussian filter. For denoising, the first five cerebro-spinal fluid and white matter principal components were used as nuisance covariates in accordance with the anatomical component-based noise correction method (aCompCor).[27] The six rigid motion parameters and their first temporal derivatives were regressed out from data. Outliers detected by the ART toolbox (if any) and spurious effects from the first two time-points (to maximize magnetic equilibrium) were also regressed out from data. Finally, resting state fMRI time series were linearly detrended and band-pass filtered (0.01-0.1 Hz).

Centrality analysis

Degree centrality, hereafter defined as centrality, represents the total number of connections for each voxel with any other voxel of the brain, hence providing a simple, directly quantifiable measure of network topography. We calculated binary centrality maps using the "REST-DC" toolkit embedded in the REST V1.8 package (http://www.restfmri.net). Centrality of each voxel of the brain was quantified by means of voxel-wise Pearson's correlation analysis with any other voxel of the grey matter. In order to exclude from centrality analysis voxels belonging to white matter areas and/or voxels without a reliable resting state fMRI signal, we masked the resting state fMRI

images with the corresponding grey matter masks, obtained by thresholding a standard grey matter probability atlas in the Montreal Neurological Institute space (available in SPM12 software) at 0.20. Voxel-level centrality was obtained as the sum of voxels having a significant connection with the given voxel; to this aim, only positive correlation coefficients higher than 0.25 were considered, to avoid weak correlations and spurious contributions.[13] Finally, centrality maps were converted through Fisher's Z-transformation, to account for the effect of individual variability.[10]

Statistical analysis

Statistical analyses were performed using the Stata software (version 13; StataCorp LP, College Station, TX). Demographic, clinical and MRI features of study subjects were presented as means, medians or proportions as appropriate. All demographic, clinical and MRI variables were checked for normality using the Shapiro-Wilk normality test. Differences between controls and patients with MS for demographic, clinical and structural MRI measures were assessed using generalised linear mixed-effects models adjusted for age and sex, accounting for scanner heterogeneity and clustering (participants within sites) using random intercepts. Similar models were applied to test between-phenotypes differences with the following *post hoc* contrasts, based on disease clinical evolution (i.e., MS onset is either CIS or PPMS; CIS evolves to RRMS and RRMS can evolve to SPMS; SPMS and PPMS represent the two progressive forms of the disease): CIS *vs* controls, PPMS *vs* controls, CIS *vs* PPMS, RRMS *vs* CIS, SPMS *vs* RRMS, and PPMS *vs* SPMS. False discovery rate method was applied to correct for multiple comparison.[28] Second-level voxel-wise statistics for centrality were performed using SPM12, including age, sex, scanner, framewise displacement and normalised grey matter volume as confounding covariates. Comparisons of centrality maps between controls and patients with MS, as well as among MS phenotypes, were performed using analysis of variance (ANOVA) models, as implemented in SPM12. For phenotype comparisons, the same *post hoc* contrasts used for clinical/structural MRI variables were used. ANOVA models were also used to compare controls, cognitively preserved and cognitively impaired patients with MS. To identify specific centrality abnormalities for cognitively impaired *vs both* cognitively preserved patients

with MS and controls, we performed a conjunction analysis.[29] Finally, correlations between centrality maps and EDSS, T2 lesion volume and normalised brain/grey matter volumes were assessed through linear regression models including age, sex and scanner as confounding covariates. Second-level SPM12 analyses were tested at $p<0.05$, cluster-wise family-wise error (FWE) to account for multiple comparisons. We also identified results surviving at $p<0.001$ (uncorrected, cluster extent threshold k=10 voxels).

Data availability

The anonymised dataset used and analysed during the current study is available from the corresponding author upon reasonable request.

Results

Clinical, neuropsychological, and structural MRI measures

We screened 1003 patients with MS and 355 controls for inclusion in the study. After exclusion of 32 patients and 25 controls due to poor image quality (n=8/10 controls/patients) and post-processing failure (excessive movement: n=11/15 controls/patients; misregistration: n=6/7 controls/patients), 1301 subjects were finally included in the study. Demographic, clinical and structural MRI data from these subjects are summarized in Table 1. There were 330 controls and 971 patients with MS, including 47 CIS, 704 RRMS, 145 SPMS and 75 PPMS. Compared to controls, patients with MS showed lower normalised brain ($p<0.001$) and grey matter ($p<0.001$) volumes.

Overall, patients with CIS and RRMS were younger compared with controls ($p=0.001$ and $p=0.03$, respectively) while patients with SPMS and PPMS were older compared with controls ($p=0.03$ and $p=0.001$, respectively).

Thirty-nine % of patients with MS were cognitively impaired. Patients with RRMS and PPMS showed higher prevalence of cognitive impairment *vs* patients with CIS (36% and 53% *vs* 19%, $p<0.003$). Patients with SPMS showed higher prevalence of cognitive impairment compared with RRMS (53% *vs* 36%, $p=0.001$). No differences were found when comparing prevalence of cognitive impairment in patients with PPMS *vs* SPMS.

Patients with CIS did not differ from controls for T2 lesion volume, normalised brain/grey matter volumes. Patients with PPMS showed lower normalised brain (p=0.001) and grey matter volumes (p=0.001) *vs* controls. Compared to patients with CIS, patients with RRMS and PPMS had higher T2 lesion volume (p range 0.002–0.009), lower normalised brain (all p=0.001) and grey matter (p range 0.002–0.009) volumes. Compared to patients with RRMS, patients with SPMS had higher T2 lesion volume (p=0.001), lower normalised brain (p=0.001) and grey matter (p=0.001) volumes. Finally, compared to patients with PPMS, patients with SPMS had higher T2 lesion (p=0.001) and lower normalised brain volume (p=0.007).

Centrality analysis: Patients with MS *vs* controls

Results of the between-group comparison of centrality between patients with MS and controls are outlined in Figure 1 and Table 2. Compared with controls, patients with MS showed reduced centrality in the bilateral insula, bilateral paracentral lobule, bilateral caudate nucleus, bilateral postcentral gyrus and left inferior parietal gyrus, as well as increased centrality in the bilateral precuneus and middle occipital gyrus ($p<0.05$, FWE corrected). At uncorrected threshold ($p<0.001$), they also showed reduced centrality in the left superior temporal gyrus, right cerebellum, left parahippocampal gyrus and hippocampus, and bilateral thalamus, as well as increased centrality in several bilateral middle/superior frontal regions, right parahippocampal gyrus, and right middle cingulate and olfactory cortex.

Centrality and MS phenotypes

Table 3 and Figure 2 summarize results of centrality comparisons among MS phenotypes (all results surviving at $p<0.001$, uncorrected, unless otherwise specified). Patients with CIS showed reduced centrality in insular, occipital and temporal regions, as well as increased centrality in the precuneus, middle frontal and cerebellar regions *vs* controls. Patients with PPMS showed similar, but more extensive centrality abnormalities, in addition to reduced centrality in the bilateral paracentral lobule, precentral gyrus, middle occipital and lingual gyrus, and caudate nucleus, and increased centrality in orbitofrontal and superior frontal regions *vs* controls. Patients with RRMS patients

showed reduced centrality in the bilateral caudate nucleus and thalamus, as well as increased centrality in the bilateral middle temporal gyrus *vs* patients with CIS.

Patients with SPMS exhibited a widespread reduction of centrality *vs* patients with RRMS in regions of the sensorimotor system, in the bilateral insula, middle cingulate cortex and right thalamus, as well as in the right anterior cingulate cortex. They also had increased centrality in the right precuneus ($p<0.05$, FWE), bilateral occipital regions, right orbitofrontal cortex, hippocampus and bilateral temporal regions ($p<0.05$, FWE) *vs* patients with RRMS.

Compared to patients with PPMS, patients with SPMS showed reduced centrality in parietal, frontal and cerebellar regions, as well as increased centrality in occipital and frontal regions. Finally, patients with PPMS showed reduced centrality in fronto-temporal regions and increased centrality in parietal and supplementary motor regions *vs* patients with CIS.

Centrality and cognitive impairment

Table 4 summarises results of centrality comparisons according to patients' cognitive status. Compared with controls, both cognitively preserved and cognitively impaired patients with MS showed patterns of abnormal centrality similar to those detected in the whole-MS group (data not shown). In a conjunction analysis, cognitively impaired patients with MS showed a decrease of centrality in the right insula and left paracentral lobule, as well as an increase of centrality in the left middle occipital gyrus and right middle temporal cortex *vs* both controls and cognitively preserved patients with MS ($p<0.001$, uncorrected at conjunction analysis).

Correlation analysis in patients with MS

A higher EDSS was associated with increased centrality in the right precuneus ($r=0.20$, $p<0.05$, FWE). At an uncorrected threshold, higher EDSS also correlated with increased centrality in the right middle frontal gyrus ($r=0.16$, $p<0.001$) and with decreased centrality in the left postcentral gyrus ($r=-0.18$, $p<0.001$).

Higher T2 lesion volume was associated with reduced centrality of the left thalamus ($r=-0.19$, $p<0.05$ FWE), right insula ($r=-0.18$, $p<0.001$), left caudate nucleus ($r=-0.18$, $p<0.001$), and of

several cerebellar regions (r=range -0.17/-0.15, p<0.05 FWE) (Table 5). In addition, lower normalized brain volume was associated with reduced centrality of the bilateral insula (left: r=0.26; right: r=0.26; p<0.05 FWE), right cerebellum (r=range 0.27-0.28, p<0.05 FWE) and right superior frontal gyrus (r=0.24, p<0.05 FWE) and increased centrality of the left precuneus (r=-0.29, p<0.05 FWE) and right middle cingulate cortex (r=-0.29, p<0.05 FWE). Lower grey matter volume was associated with reduced centrality of the bilateral insula (left: r=0.25; right: r=0.26; p<0.05 FWE) and bilateral cerebellum (left: r=0.22, right: 0.23; p<0.05 FWE) and increased centrality of the bilateral precuneus (right: r=-0.21; left: r=-0.24, p<0.05 FWE), bilateral middle cingulate cortex (right: -0.28, left: -0.31, p<0.05 FWE), and inferior frontal gyrus (r=-0.21, p<0.001) (Table 5).

Discussion

In this study, we assessed brain functional network topography abnormalities across MS phenotypes in a large, multi-centre sample using voxel-wise centrality. We also sought to explore the association between centrality abnormalities and clinical, cognitive and MRI features. Overall, we found that patients with MS had reduced centrality in regions belonging to the salience network (e.g. bilateral insula) and to the sensorimotor network (e.g. bilateral pre- and post-central gyri and caudate nucleus) as well as increased centrality in regions belonging to the default mode network (e.g., precuneus) compared with controls. Centrality abnormalities were already detected in patients with CIS, but were more pronounced and widespread in patients with progressive phenotypes. These abnormalities mirrored clinical disability and cognitive impairment and showed significant associations with MRI measures of structural damage.

Voxel-wise centrality is a measure of brain network topography reflecting, at voxel-level, the functional importance of a given voxel over the whole brain networks. Centrality has been already employed to explore resting state functional network topography alterations in several neurodegenerative conditions. Specific patterns of centrality abnormalities were described for each condition, with Parkinson's disease characterised by reduced centrality in fronto-temporal areas and

increased default mode network centrality,[30, 31] Alzheimer's disease characterised by reduced centrality in temporal areas and increased centrality in frontal regions,[31-33] and systemic lupus erythematosus characterised by reduced centrality in the parietal lobe and increased centrality in the insula-hippocampal cortices.[34] Such specificity in centrality abnormalities illustrates the potential value of centrality analysis in MS, a complex disease that needs specific correlates of the different pathophysiological processes occurring across different stages.

In line with previous studies[8, 12, 13, 16] in our study we detected in patients with MS a reduced centrality in sensorimotor and salience network, as well as an increased centrality in the default mode network. The three networks showing most abnormalities (i.e., the sensorimotor, salience and default-mode networks) are highly interconnected with the salience network regulating the switch between networks internally (default mode network) and externally oriented (control network, motor network and visual network). In patients with MS, salience network damage may produce a less flexible, less agile and less efficient brain network reconfiguration and integration when subjects are exposed to external stimuli leaving patients more vulnerable to demanding motor and cognitive tasks.

One of the main strengths of the present study was the assessment of centrality in the different MS phenotypes. Our results revealed a circumscribed decrease of centrality in insular and temporal regions, together with precuneus centrality increase in patients at their first clinical demyelinating event, namely CIS, *vs* controls. This finding confirms that subtle centrality alterations in the salience and default mode networks occur since early disease stages. However, when the diagnosis of MS is drawn, more extensive and specific centrality abnormalities were detected. Patients with RRMS were characterised by a reduced centrality in the bilateral caudate nucleus and thalamus, and by an increased centrality in frontal and temporal cortices compared with patients with CIS. A reduced centrality in deep grey matter is in line with previous findings obtained using resting state functional connectivity analysis[6] and suggests that impaired network integration, especially involving the deep grey matter, may be crucial in the RRMS phase of the disease. Moving to

progressive phenotypes, both patients with PPMS and SPMS were characterized by a more diffuse and marked centrality decrease in several regions belonging to the sensorimotor and salience networks (including cortical and subcortical structures), and by a widespread centrality increase of anterior and posterior default mode network areas. Possibly, early over the disease course functional reorganization counteracts structural damage up to a tipping point when functional derangement becomes less efficient.[8] This tipping point might correspond to the evolution from relapsing to progressive phenotypes with sub-cortical structures being less connected with cortical hubs, resulting in a deregulation of proper switch between network configuration according to internal and external stimuli.[35, 36] Hence, according to preliminary findings from a longitudinal study,[15] network centrality may represent an useful biomarker to identify patients with the highest risk for clinical progression. Notwithstanding the findings here reported, we do also acknowledge that both CIS and PPMS groups were smaller compared with other groups (controls, patients with RRMS and SPMS) and hence, our results could have underestimated centrality changes occurring in patients with CIS and PPMS. Future studies selectively focusing on these MS phenotypes are needed to confirm our findings.

Given the large sample size, we were also able to explore the association between centrality abnormalities and cognitive impairment. Cognitively impaired patients with MS had reduced centrality in the salience network and increased centrality in parieto-temporal regions of the default mode network compared to both patients without cognitive impairment and controls. Previous centrality analyses consistently found an increased centrality of the default mode network in patients with MS with impaired cognitive abilities.[12, 15, 16] The default mode network is an internally oriented network, which needs to be deactivated to properly process external stimuli.[37] This de-activation of the default mode network during specific tasks is hampered in MS.[38] Hence, brain networks stuck in a configuration unable to process cognitive stimuli swiftly and appropriately.

When looking at the direct association between centrality abnormalities and clinical disability, we found that more severe EDSS score was associated with increased centrality of the right precuneus

(at corrected threshold) and decreased centrality of the left postcentral gyrus (at uncorrected threshold). While the latter association is not surprising, given that physical disability measured through the EDSS is highly reflective of the motor and sensory function in patients with MS,[20] the association between centrality in the right precuneus and EDSS is less straightforward. Precuneus activation measured with task-based fMRI has been associated with motor preparation especially when asking patient to voluntary move an impaired limb.[39] Probably, a higher extent of physical disability produces a more complex recruitment of cognitive networks in the attempt to plan motor alternative strategies to fulfil tasks demand.

Higher T2-hyperintense lesion volume correlated with decreased thalamic and cerebellar centrality. This association suggests that centrality abnormalities in MS may be due to a structural disconnection. Noteworthy, centrality abnormalities mostly involved two structures highly connected with cortical areas by means of long-range direct and indirect structural connections, namely the thalamus[40] and the cerebellum.[41] Long-range connections are more widely damaged in MS compared with short-range connection,[42] possibly underpinning a structural-functional decupling ultimately resulting in a lower number of functional connections, that is a reduced centrality. Assessing the association between brain atrophy and centrality, we observed that lower normalised brain and grey matter volumes were associated with reduced centrality in the salience network, and increased centrality in the default mode network, which were, in turn, associated with cognitive impairment in our sample. Therefore, we could argue that neurodegeneration may fuel centrality abnormalities ultimately leading to cognitive disability.

We do acknowledge that this study is not without limitations. First, its cross-sectional nature prevents us to draw any conclusion about network dynamic changes over the disease course and hence, about the adaptive or maladaptive role of centrality changes. Given the large sample size and the inclusion of patients spanning the main disease clinical phenotypes, our analysis indirectly assessed the roadmap of centrality changes throughout different MS stages. Second, cognitive impairment was assessed at a global level using a standardized battery. However, subtle cognitive

deficits, i.e., social cognition and metacognition deficits, may occur in these patients and may not be captured through the applied cognitive battery. Third, the presence of extensive atrophy may bias centrality calculation, although centrality changes have been reported in patients without atrophy as well.[36] However, we used a grey matter mask to exclude spurious contributions from other tissues, and we counted as significant connections only Pearson's correlations exceeding r=0.25. This is a stringent threshold and, given the quite aggressive post-processing performed on our data, including the careful removal of several sources of spurious signal, we believe that only true grey matter voxels are contributing to centrality maps. However, in order to not miss possible relevant results, we showed findings at both corrected and uncorrected threshold. Furthermore, we included normalized grey matter volume as a covariate to correct for spurious effects from partial volume. Fourth, because of the stringent correlation threshold for centrality maps construction, we only included positive functional connections in centrality maps and not negative correlations. Indeed, the role of negative correlations is still not clear and debated among neuroscientists.[43-45] Finally, to unveil pathological substrates underpinning centrality changes, a more comprehensive MRI assessment including regional grey matter volume, cortical lesions and white matter tracts with diffusion-weighted images (not available for this dataset) may contribute to better capture structural-functional intermingled damages.

To conclude, in this multi-centre study exploring functional network topography in a large sample of patients using a voxel-wise centrality approach, we observed that patients with MS presented with reduced network centrality in primary sensorimotor and salience networks, and increased centrality in the default mode network. Centrality alterations start from selected cortico-subcortical regions in CIS and progressively spread to larger areas in patients with RRMS and SPMS. Collectively, increased centrality in the default mode network and frontal areas may represent useful biomarkers to identify patients presenting severe physical disability and cognitive deficits.

Appendix 1. Authors

Name	Location	Role	Contribution
Antonio Carotenuto, MD	IRCCS San Raffaele Scientific Institute, Milan, Italy	Author	Analysis and interpretation of the data, and drafting/revising the manuscript
Paola Valsasina, MSc	IRCCS San Raffaele Scientific Institute, Milan, Italy	Author	Analysis and interpretation of the data, and drafting/revising the manuscript
Menno M Schoonheim, PhD	Department of Anatomy and Neurosciences, MS Center Amsterdam, Amsterdam Neuroscience, Amsterdam UMC, Vrije Universiteit Amsterdam, Amsterdam, The Netherlands	Author	Data collection, interpretation of the data and drafting/revising the manuscript
Jeroen J G Geurts, PhD	Department of Anatomy and Neurosciences, MS Center Amsterdam, Amsterdam Neuroscience, Amsterdam UMC, Vrije Universiteit Amsterdam, Amsterdam, The Netherlands	Author	Data collection and drafting/revising the manuscript
Frederik Barkhof, MD, PhD	Radiology and Nuclear Medicine, MS Center Amsterdam, Amsterdam Neuroscience, Amsterdam UMC, Vrije Universiteit Amsterdam, Amsterdam, The Netherlands, Institutes of Neurology & Healthcare Engineering, UCL, National Institute for health research (NIHR) University College London Hospitals (UCLH) Biomedical research centre, London, UK	Author	Data collection and drafting/revising the manuscript
Antonio Gallo, MD, PhD	Division of Neurology and 3T MRI Research Center, Department of Advanced Medical and Surgical Sciences, University of Campania “Luigi Vanvitelli”, Naples, IT, Italy	Author	Data collection and drafting/revising the manuscript
Gioacchino Tedeschi, MD	Division of Neurology and 3T MRI Research Center, Department of Advanced Medical and Surgical Sciences, University of Campania “Luigi	Author	Data collection and drafting/revising the manuscript

	Vanvitelli", Naples, IT, Italy		
Silvia Tommasin, PhD	Department of Human Neurosciences, Sapienza University, Rome, Italy	Author	Data collection and drafting/revising the manuscript
Patrizia Pantano, MD, PhD	Department of Human Neurosciences, Sapienza University, Rome, IRCCS NEUROMED, Pozzilli, (IS) Italy	Author	Data collection, interpretation of the data and drafting/revising the manuscript
Massimo Filippi, MD	IRCCS San Raffaele Scientific Institute, Vita-Salute San Raffaele University, Milan, Italy	Author	Drafting/revising the manuscript, and analysis and interpretation of the data.
Maria A. Rocca, MD	IRCCS San Raffaele Scientific Institute, Milan, Italy. Vita-Salute San Raffaele University	Corresponding author	Study concept, analysis and interpretation of the data, drafting/revising the manuscript. Study supervisor.

Appendix 2. Coinvestigators

Name	**Location**	**Role**	**Contribution**
Jaume Sastre-Garriga, MD	Hospital Universitari Vall d'Hebron, Universitat Auto`noma de Barcelona, Spain	Coinvestigator	Study design and interpretation of the data
Olga Ciccarelli, MD, PhD	UCL Institute of Neurology, London, UK	Coinvestigator	Study design and interpretation of the data
Nicola De Stefano, MD, PhD	University of Siena, Italy	Coinvestigator	Study design and interpretation of the data
Christian Enzinger, MD, PhD	Department of Neurology, Medical University of Graz, Austria	Coinvestigator	Study design and interpretation of the data
Claudio Gasperini, MD, PhD	San Camillo-Forlanini Hospital, Rome, Italy	Coinvestigator	Study design and interpretation of the data
Ludwig Kappos, MD, PhD	University of Basel, Switzerland	Coinvestigator	Study design and interpretation of the data
Jacqueline Palace, MD, PhD	University of Oxford, UK	Coinvestigator	Study design and interpretation of the data
Alex Rovira, MD, PhD	Hospital Universitari Vall d'Hebron, Barcelona, Spain	Coinvestigator	Study design and interpretation of the data
Hugo Vrenken, PhD	VU University Medical Author Centre, Amsterdam, the Netherlands	Coinvestigator	Study design and interpretation of the data
Tarek Yousry, MD, PhD	Queen Square MS Centre, UCL Institute of Neurology, London UK	Coinvestigator	Study design and interpretation of the data

References

1. Filippi M, Bar-Or A, Piehl F, et al. Multiple sclerosis. Nat Rev Dis Primers 2018;4:43.
2. Rao SM, Leo GJ, Bernardin L, Unverzagt F. Cognitive dysfunction in multiple sclerosis. I. Frequency, patterns, and prediction. Neurology 1991;41:685-691.
3. Rocca MA, Colombo B, Falini A, et al. Cortical adaptation in patients with MS: a cross-sectional functional MRI study of disease phenotypes. Lancet Neurol 2005;4:618-626.
4. Filippi M, Rocca MA, Barkhof F, et al. Association between pathological and MRI findings in multiple sclerosis. Lancet Neurol 2012;11:349-360.
5. Chard DT, Alahmadi AAS, Audoin B, et al. Mind the gap: from neurons to networks to outcomes in multiple sclerosis. Nat Rev Neurol 2021;17:173-184.
6. Rocca MA, Valsasina P, Leavitt VM, et al. Functional network connectivity abnormalities in multiple sclerosis: Correlations with disability and cognitive impairment. Mult Scler 2018;24:459-471.
7. Rocca MA, Valsasina P, Absinta M, et al. Default-mode network dysfunction and cognitive impairment in progressive MS. Neurology 2010;74:1252-1259.
8. Schoonheim MM, Meijer KA, Geurts JJ. Network collapse and cognitive impairment in multiple sclerosis. Front Neurol 2015;6:82.
9. Rubinov M, Sporns O. Complex network measures of brain connectivity: uses and interpretations. Neuroimage 2010;52:1059-1069.
10. Zuo XN, Ehmke R, Mennes M, et al. Network centrality in the human functional connectome. Cereb Cortex 2012;22:1862-1875.
11. Schoonheim MM, Geurts J, Wiebenga OT, et al. Changes in functional network centrality underlie cognitive dysfunction and physical disability in multiple sclerosis. Mult Scler 2014;20:1058-1065.
12. Dekker I, Schoonheim MM, Venkatraghavan V, et al. The sequence of structural, functional and cognitive changes in multiple sclerosis. Neuroimage Clin 2021;29:102550.
13. Zhuang Y, Zhou F, Gong H. Intrinsic functional plasticity of the sensorimotor network in relapsing-remitting multiple sclerosis: evidence from a centrality analysis. PLoS One 2015;10:e0130524.
14. Koubiyr I, Deloire M, Besson P, et al. Longitudinal study of functional brain network reorganization in clinically isolated syndrome. Mult Scler 2020;26:188-200.
15. Huiskamp M, Eijlers AJC, Broeders TAA, et al. Longitudinal Network Changes and Conversion to Cognitive Impairment in Multiple Sclerosis. Neurology 2021;97:e794-e802.

16. Eijlers AJ, Meijer KA, Wassenaar TM, et al. Increased default-mode network centrality in cognitively impaired multiple sclerosis patients. Neurology 2017;88:952-960.
17. Oldfield RC. The assessment and analysis of handedness: the Edinburgh inventory. Neuropsychologia 1971;9:97-113.
18. Toga AW, Thompson PM. Mapping brain asymmetry. Nat Rev Neurosci 2003;4:37-48.
19. Thompson AJ, Banwell BL, Barkhof F, et al. Diagnosis of multiple sclerosis: 2017 revisions of the McDonald criteria. Lancet Neurol 2018;17:162-173.
20. Kurtzke JF. Rating neurologic impairment in multiple sclerosis: an expanded disability status scale (EDSS). Neurology 1983;33:1444-1452.
21. Amato MP, Portaccio E, Goretti B, et al. The Rao's Brief Repeatable Battery and Stroop Test: normative values with age, education and gender corrections in an Italian population. Mult Scler 2006;12:787-793.
22. Amato MP, Morra VB, Falautano M, et al. Cognitive assessment in multiple sclerosis-an Italian consensus. Neurol Sci 2018;39:1317-1324.
23. Valverde S, Cabezas M, Roura E, et al. Improving automated multiple sclerosis lesion segmentation with a cascaded 3D convolutional neural network approach. Neuroimage 2017;155:159-168.
24. Battaglini M, Jenkinson M, De Stefano N. Evaluating and reducing the impact of white matter lesions on brain volume measurements. Hum Brain Mapp 2012;33:2062-2071.
25. Whitfield-Gabrieli S, Nieto-Castanon A. Conn: a functional connectivity toolbox for correlated and anticorrelated brain networks. Brain Connect 2012;2:125-141.
26. Power JD, Barnes KA, Snyder AZ, Schlaggar BL, Petersen SE. Spurious but systematic correlations in functional connectivity MRI networks arise from subject motion. Neuroimage 2012;59:2142-2154.
27. Behzadi Y, Restom K, Liau J, Liu TT. A component based noise correction method (CompCor) for BOLD and perfusion based fMRI. Neuroimage 2007;37:90-101.
28. Hochberg Y. A Sharper Bonferroni Procedure for Multiple Tests of Significance. Biometrika 1988;75:800-802.
29. Friston KJ, Holmes AP, Price CJ, Buchel C, Worsley KJ. Multisubject fMRI studies and conjunction analyses. Neuroimage 1999;10:385-396.
30. Jin C, Qi S, Teng Y, et al. Altered Degree Centrality of Brain Networks in Parkinson's Disease With Freezing of Gait: A Resting-State Functional MRI Study. Front Neurol 2021;12:743135.

31. Zhou J, Li K, Luo X, et al. Distinct impaired patterns of intrinsic functional network centrality in patients with early- and late-onset Alzheimer's disease. Brain Imaging Behav 2021;15:2661-2670.
32. Ng ASL, Wang J, Ng KK, et al. Distinct network topology in Alzheimer's disease and behavioral variant frontotemporal dementia. Alzheimers Res Ther 2021;13:13.
33. Luo Y, Sun T, Ma C, et al. Alterations of Brain Networks in Alzheimer's Disease and Mild Cognitive Impairment: A Resting State fMRI Study Based on a Population-specific Brain Template. Neuroscience 2021;452:192-207.
34. Wang Y, Jiang M, Huang L, et al. Altered Functional Brain Network in Systemic Lupus Erythematosus Patients Without Overt Neuropsychiatric Symptoms Based on Resting-State Functional Magnetic Resonance Imaging and Multivariate Pattern Analysis. Front Neurol 2021;12:690979.
35. d'Ambrosio A, Valsasina P, Gallo A, et al. Reduced dynamics of functional connectivity and cognitive impairment in multiple sclerosis. Mult Scler 2020;26:476-488.
36. Eijlers AJC, Wink AM, Meijer KA, Douw L, Geurts JJG, Schoonheim MM. Reduced Network Dynamics on Functional MRI Signals Cognitive Impairment in Multiple Sclerosis. Radiology 2019;292:449-457.
37. Raichle ME, MacLeod AM, Snyder AZ, Powers WJ, Gusnard DA, Shulman GL. A default mode of brain function. Proc Natl Acad Sci U S A 2001;98:676-682.
38. Rocca MA, Valsasina P, Hulst HE, et al. Functional correlates of cognitive dysfunction in multiple sclerosis: A multicenter fMRI Study. Hum Brain Mapp 2014;35:5799-5814.
39. Cojan Y, Waber L, Schwartz S, Rossier L, Forster A, Vuilleumier P. The brain under self-control: modulation of inhibitory and monitoring cortical networks during hypnotic paralysis. Neuron 2009;62:862-875.
40. Minagar A, Barnett MH, Benedict RH, et al. The thalamus and multiple sclerosis: modern views on pathologic, imaging, and clinical aspects. Neurology 2013;80:210-219.
41. Marek S, Siegel JS, Gordon EM, et al. Spatial and Temporal Organization of the Individual Human Cerebellum. Neuron 2018;100:977-993 e977.
42. Meijer KA, Steenwijk MD, Douw L, Schoonheim MM, Geurts JJG. Long-range connections are more severely damaged and relevant for cognition in multiple sclerosis. Brain 2020;143:150-160.
43. Chang C, Glover GH. Effects of model-based physiological noise correction on default mode network anti-correlations and correlations. Neuroimage 2009;47:1448-1459.

44. Fox MD, Zhang D, Snyder AZ, Raichle ME. The global signal and observed anticorrelated resting state brain networks. J Neurophysiol 2009;101:3270-3283.
45. Van Dijk KR, Hedden T, Venkataraman A, Evans KC, Lazar SW, Buckner RL. Intrinsic functional connectivity as a tool for human connectomics: theory, properties, and optimization. J Neurophysiol 2010;103:297-321.

Table 1. Clinical and structural MRI features of controls and patients with multiple sclerosis (MS). Patients are first considered as a whole and then divided according to disease phenotype.

	Controls	MS	p*	CIS	RRMS	SPMS	PPMS	p*
Subjects	330	971	-	47	704	145	75	-
Female/Male, n	186/144	624/347	0.01	28/19	476/228	86/59	34/41	0.001
Age, mean ± SD (years)	41.2 ± 13.3	43.1 ± 11.8	0.22	32.2 ± 8.6	40.7 ± 10.7	51.8 ± 9.6	55.1 ± 9.9	<0.001
Milan (1st scanner), n	32	255		11	167	54	23	
Milan (2nd scanner), n	69	78		3	51	14	10	
Amsterdam, n	96	332	<0.001	0	244	52	36	<0.001
Naples,	101	199		28	150	17	4	
Rome, n	32	107		5	92	8	2	
EDSS, median (range)	-	2.5 (0 - 8.5)	-	1 (0 - 2)	2 (0 - 7.5)	6 (2 - 8)	6 (4 - 8.5)	<0.001
Disease duration, median (range) (years)	-	10 (0 - 46)	-	1 (0 - 5)	9 (0 - 40)	19 (0 - 46)	13 (2 - 45)	0.001
Cognitively preserved/Cognitively impaired, n	-	590/381	-	38/9	449/255	68/77	35/40	0.03
T2 lesion volume, mean ± SD (mL)	3.2 ± 6.6	10.3 ± 11.5	0.001	2.4 ± 3.0	8.8 ± 9.4	18.1 ± 16.2	13.2 ± 13.1	<0.001
Normalised brain volume, mean ± SD (mL)	1550 ± 66	1507 ± 88	<0.001	1598 ± 84	1517 ± 84	1451 ± 75	1457 ± 83	<0.001
Normalised grey matter volume, mean ± SD (mL)	851 ± 70	811 ± 75	<0.001	881 ± 66	824 ± 68	761 ± 73	758 ± 73	<0.001

*Linear mixed-effect model accounting for clustering (participants within sites)

Abbreviations: MS=Multiple Sclerosis; CIS=Clinically isolated syndrome; RRMS=Relapsing-remitting multiple sclerosis; SPMS=Secondary progressive multiple sclerosis; PPMS=Primary progressive multiple sclerosis; EDSS= Expanded disability status scale

Table 2. Degree centrality abnormalities in patients with multiple sclerosis compared with controls. Data obtained using SPM12 and ANOVA models, age-, sex-, scanner-, framewise displacement and normalised grey matter volume adjusted. Results were significant at $p<0.001$, uncorrected (cluster extent k=10 voxels). Results surviving at $p<0.05$, cluster-wise family-wise error corrected, are marked with *.

Region	MNI coordinates			K	T value
	x	y	z		
Reduced centrality in patients with MS *vs* controls					
R Insula*	36	-20	14	345	5.98
L Insula*	-40	-10	6	81	4.41
B PaCL*	-2	-32	64	817	5.16
	8	-28	58		4.68
L Caudate Nucleus*	-10	12	16	112	5.48
R Caudate Nucleus*	10	10	16	112	5.11
R Postcentral gyrus*	60	-14	40	532	4.50
L Postcentral gyrus	-54	10	22	53	3.80
L IPG*	-46	-26	44	297	4.54
L STG	-42	-30	14	55	4.03
L PHG	-28	-16	-26	47	4.26
L Hippocampus	-24	-32	-4	20	3.86
L Thalamus	-8	-22	12	10	3.77
R Thalamus	10	-26	12	17	3.95
R Cerebellum (lobule IV/V)	8	-44	-8	71	4.15
R Cerebellum (vermis)	6	-56	-4	71	3.48
Increased centrality in patients with MS *vs* controls					
R Precuneus*	18	-56	28	120	5.50
L Precuneus*	-18	-62	30	104	3.86
L MOG*	-32	-70	30	500	4.92
R MOG*	36	-62	30	121	4.75
R MTG	38	-60	12	23	4.60
L IFG	-32	22	-20	26	3.82
L SFG	-22	48	-10	19	4.30
R SFG	24	46	10	50	4.83
R PHG	10	-4	-26	31	4.12
R Olfactory	2	20	-14	67	4.36
L Precuneus	-14	-46	42	76	4.45
R MFG	28	50	-8	41	4.02
L MFG	-32	10	44	42	4.26
R MCC	14	12	40	18	4.17

R Cerebellum (crus II)	50	-46	-42	24	4.03

Abbreviations: MS=multiple sclerosis; L=left; R=right; B=Bilateral; IPG=inferior parietal gyrus; MTG=middle temporal gyrus; STG=superior temporal gyrus; PaCL=Paracentral lobule; PHG=parahippocampal gyrus; IFG=inferior frontal gyrus; MFG=middle frontal gyrus; SFG=superior frontal gyrus; MOG=middle occipital gyrus; MCC=middle cingulate cortex.

Table 3. Degree centrality abnormalities in patients with multiple sclerosis according to disease clinical phenotype. Data obtained using SPM12 and ANOVA models with *post hoc* contrasts, age-, sex-, scanner-, framewise displacement and normalised grey matter volume adjusted. Results were significant at p<0.001, uncorrected (cluster extent k=10 voxels). Results surviving at p<0.05, cluster-wise family-wise error corrected, are marked with *.

CIS *vs* controls		PPMS *vs* controls		PPMS *vs* CIS		RRMS *vs* CIS		SPMS *vs* RRMS		SPMS *vs* PPMS	
Region	**T value**	**Region**	**T value**	**Region**	**T value**	**Region**	**T value**	**Region**	**T value**	**Region**	**T value**
Reduced centrality											
R Insula	3.69	R Insula*	5.89					R Insula	3.89		
		L Insula	4.32					L Insula	4.15		
		R PaCL	3.49								
		L PaCL	3.76	L PaCL	3.67						
				R MCC	3.89			R MCC	4.12		
								L MCC	4.51		
										R SPG	4.10
		R MOG	3.95								
				L Calcarine	4.03						
		R Calcarine	3.65								
		L LING*	3.92								
R IOG	3.37	R IOG	3.69								
				L IPG	4.19						
		R PreCG	3.49								
		L PreCG	3.78								
								R ACC*	3.85		
								L IFG	3.44	L IFG	4.47
								R STG	4.09		
L STG	3.82										
L MTG	3.77							L MTG	3.93		
		R MTG	3.69								
		R Caudate	4.68	R Caudate	3.54	R Caudate	3.86				
		L Caudate	4.09			L Caudate	3.73				

						R Thalamus L Thalamus R Cer lob VII	3.59 3.71 3.37	R Thalamus	3.86	R Cer cr II	4.60
Increased centrality											
R Precuneus	4.18	L MOG L SMG	3.83 4.22	R SMG	3.55			R Precuneus* R MOG	4.19 3.64	R LING	3.58
L MFG	3.95	L MFG L SFG R OFC L OFC	3.77 4.23 4.52 4.15	R OFC R Gyrus rectus	3.63 4.41			L ANG L MFG R MFG R OFC	4.28 4.54 3.50 4.37	L MFG R IFG	4.61 3.54
				L MTG	3.79	R MTG L MTG*	3.76 4.30	R MTG L ITG R HIPP	3.88 3.68 3.85	R HIPP	3.58
R Cer lob VII	3.98	R Cer lob X R Cer cr II R Cer lob VIII	4.05 3.80 3.77								

Abbreviations: CIS=clinically isolated syndrome; RRMS=relapsing-remitting MS; SPMS=secondary-progressive MS; PPMS=primary-progressive MS; L=left; R=right; MCC=middle cingulate cortex; ACC=anterior cingulate cortex; SMG=supramarginal gyrus; IPG=inferior parietal gyrus; SPG=superior parietal gyrus; PaCL=paracentral lobule; IOG=inferior occipital gyrus; LING=lingual gyrus; PreCG=precentral gyrus; IFG=inferior frontal gyrus; MFG=middle frontal gyrus; SFG=superior frontal gyrus; ITG=inferior temporal gyrus; MTG=middle temporal gyrus; STG=superior temporal gyrus; Cer=cerebellum; MOG=middle occipital gyrus; ANG=angular gyrus; OFC=orbitofrontal cortex; HIPP=hippocampus;

Table 4. Degree centrality abnormalities in patients with multiple sclerosis according to the presence/absence of cognitive impairment. Data obtained using SPM12 ANOVA models and *post hoc* contrasts, age-, sex-, scanner-, framewise displacement- and normalised grey matter adjusted. Results were significant at $p<0.001$, uncorrected (cluster extent k=10). Clusters in **bold** are significant at the conjunction analysis *vs* the remaining MS group and controls.

Region	MNI coordinates			K	T value
	x	y	z		
Reduced centrality in cognitively impaired *vs* cognitively preserved patients					
R Insula	42	-12	2	23	3.96
L PaCL	-2	-16	46	34	3.87
Increased centrality in cognitively impaired *vs* cognitively preserved patients					
L MOG	-34	-62	30	36	4.69
R MTG	58	-48	2	25	3.65
L IFG	-44	10	12	16	4.41

Abbreviations: L=left; R=right; MTG=middle temporal gyrus; IFG=inferior frontal gyrus; MOG=middle occipital gyrus; PaCL=paracentral lobule.

Table 5. Correlations between degree centrality abnormalities and structural MRI measures in patients with multiple sclerosis. Data obtained using SPM12 age-, sex-, framewise displacement and scanner- adjusted linear regression models. Results were significant at $p<0.001$, uncorrected (cluster extent k=10). Results surviving at $p<0.05$, cluster-wise family-wise error corrected, are marked with *.

Region	MNI coordinates			Cluster extent k	Correlation coefficient
	x	y	z		
Negative correlation between centrality and T2 lesion load					
L Thalamus*	-8	-20	14	217	-0.19
R Insula	42	-2	-8	87	-0.18
L Caudate	-12	18	8	76	-0.18
R Cerebellum Crus I*	14	-86	-26	128	-0.15
R Cerebellum – lob VII*	4	-78	-40	98	-0.17
R Cerebellum – lob IX*	0	-58	-50	123	-0.17
Positive correlation between centrality and normalised brain volume					
L Insula*	-42	-2	-4	654	0.26
R Insula*	42	-2	-6	351	0.26
R Cerebellum Crus I*	46	-44	-28	2615	0.27
R Cerebellum lob IX*	0	-58	-50	487	0.28
R SFG*	0	22	44	1161	0.24
Negative correlation between centrality and normalised brain volume					
L Precuneus*	-14	-64	38	264	-0.29
R MCC*	16	-30	50	26	-0.29
Positive correlation between centrality and normalised grey matter volume					
L Insula*	-42	6	-12	353	0.25
R Insula*	42	6	-12	152	0.26
L Cerebellum Crus I*	42	-46	-28	176	0.23
R Cerebellum lob IV-V*	-4	-58	-2	220	0.22
Negative correlation between centrality and normalised grey matter volume					
R Precuneus*	14	-54	50	383	-0.21
L Precuneus*	-16	-62	42	465	-0.24
L MCC*	-12	22	36	132	-0.31
R MCC*	14	-12	48	519	-0.28
L IFG	-36	26	20	95	-0.21

Abbreviations: L=left; R=right; MCC=middle cingulate cortex; IFG=inferior frontal gyrus; SFG=superior frontal gyrus.

Figure Legends

Figure 1. Degree centrality abnormalities in patients with multiple sclerosis compared with controls. Data obtained using SPM12 and ANOVA models, age-, sex-, scanner-, framewise displacement- and normalised grey matter volume adjusted. Results are shown at p<0.001, uncorrected (cluster extent k=10 voxels) for illustrative purposes (decreased centrality: blue-lightblue, increased centrality: red-yellow). Images are in neurological convention. Abbreviations: L=left; R=right; A=anterior; P=posterior.

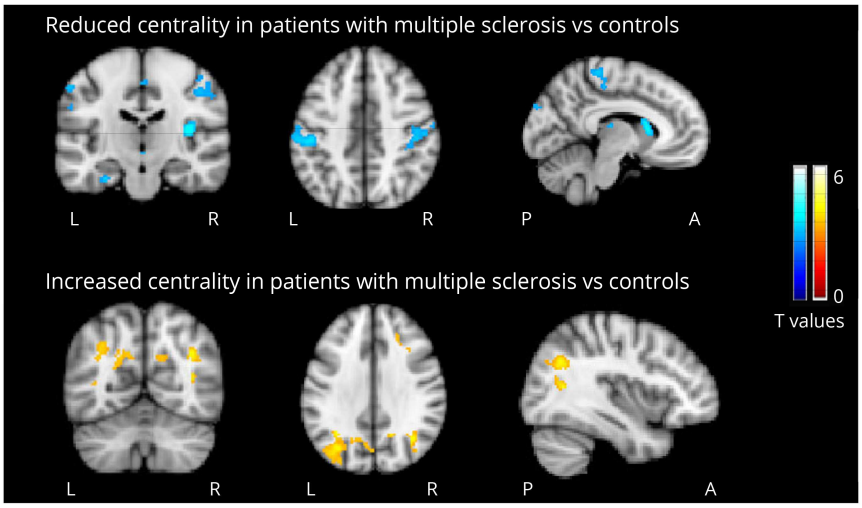

Figure 2. Degree centrality abnormalities in patients with multiple sclerosis according to disease clinical phenotype. Data obtained using SPM12 and ANOVA models with *post hoc* contrasts, age-, sex-,scanner-, framewise displacement- and normalised grey matter volume adjusted. Results are shown at p<0.001, uncorrected (cluster extent k=10 voxels) for illustrative purposes (decreased centrality: blue-lightblue, increased centrality: red-yellow). Images are in neurological convention. Abbreviations: L=left; R=right; A=anterior; P=posterior; CIS=clinically isolated syndrome; RRMS=relapsing-remitting multiple sclerosis; SPMS=secondary progressive multiple sclerosis; PPMS=primary progressive multiple sclerosis.

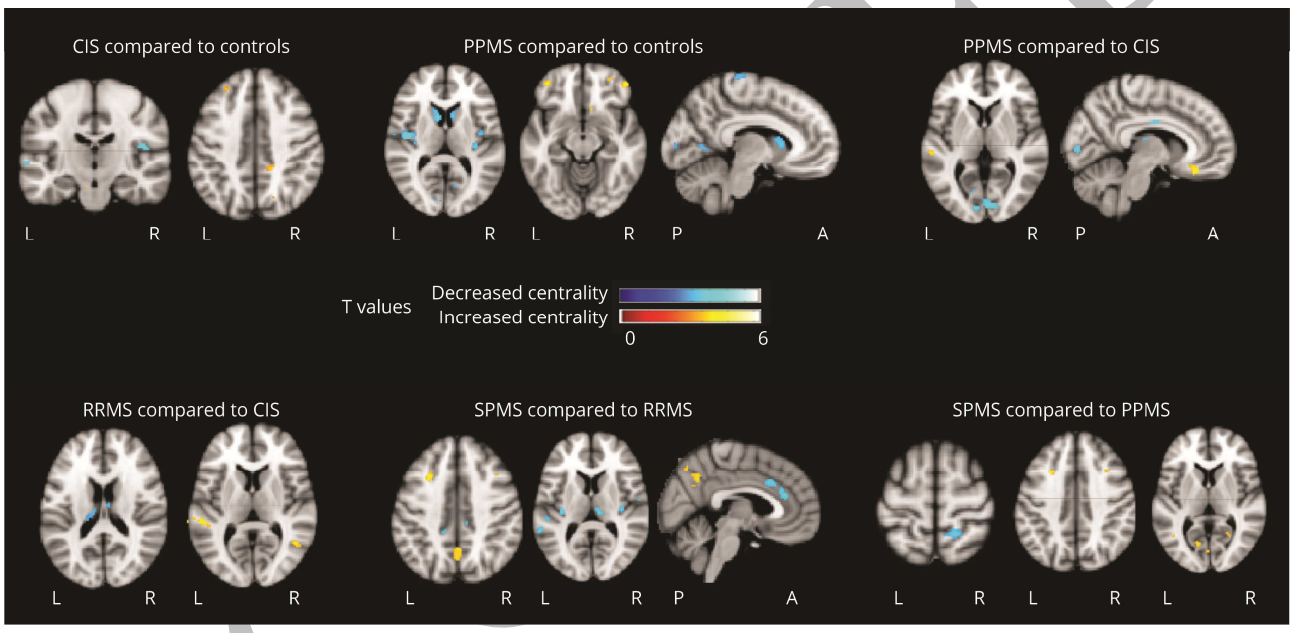

Investigating Functional Network Abnormalities and Associations With Disability in Multiple Sclerosis

Antonio Carotenuto, Paola Valsasina, Menno M. Schoonheim, et al.

Neurology published online September 12, 2022
DOI 10.1212/WNL.0000000000201264